



Multi-watt output power in-band-pumped Ho:KLu(WO₄)₂ laser

SAMI SLIMI,^{1,2} XAVIER MATEOS,²  ROSA MARIA SOLÉ,²  MAGDALENA AGUILÓ,² FRANCESC DÍAZ,² WEIDONG CHEN,^{1,3}  PAVEL LOIKO,⁴  CUI CHEN,^{1,5} UWE GRIEBNER,¹ AND VALENTIN PETROV^{1,*} 

¹Max Born Institute for Nonlinear Optics and Short Pulse Spectroscopy, Max-Born-Str. 2A, 12489 Berlin, Germany

²Universitat Rovira i Virgili (URV), Física i Cristal·lografia de Materials (FICMA), 43007 Tarragona, Spain

³Fujian Institute of Research on the Structure of Matter, Chinese Academy of Sciences, Fuzhou, 350002 Fujian, China

⁴Centre de Recherche sur les Ions, les Matériaux et la Photonique (CIMAP), UMR 6252 CEA-CNRS-ENSICAEN, Université de Caen Normandie, 6 Boulevard Maréchal Juin, 14050 Caen Cedex 4, France

⁵Research Center for Crystal Materials, Xinjiang Key Laboratory of Electronic Information Materials and Devices, Xinjiang Technical Institute of Physics & Chemistry, Chinese Academy of Sciences, Urumqi 830011, China

*petrov@mbi-berlin.de

Received 18 November 2024; revised 9 January 2025; accepted 10 January 2025; posted 10 January 2025; published 6 February 2025

Multi-watt continuous-wave operation is reported for what is believed to be the first time for an in-band-pumped Ho : KLu(WO₄)₂ laser emitting at 2078 nm in N_m polarization. The slope efficiency reached 33.5% with respect to the incident unpolarized pump radiation near 1959 nm, without pronounced roll-off effects. The total tuning range with a 1.5% output coupler covered 117 nm.

Published by Optica Publishing Group under the terms of the [Creative Commons Attribution 4.0 License](https://creativecommons.org/licenses/by/4.0/). Further distribution of this work must maintain attribution to the author(s) and the published article's title, journal citation, and DOI.

<https://doi.org/10.1364/JOSAB.549512>

1. INTRODUCTION

As laser host materials, the monoclinic potassium double tungstates with the chemical formula $KM(WO_4)_2$, where $M = Y, Gd, \text{ or } Lu$, exhibit some exceptional features that ensure the lowest lasing thresholds and highest efficiencies. These include (i) the highest absorption and emission cross-sections for trivalent rare-earth dopant ions; (ii) the largest dopant site separation among chemically simple crystals, leading to minimal interactions and concentration quenching; and (iii) the anisotropy of the spectroscopic properties, alleviating a fundamental limitation due to the relationship between radiative lifetime and integral emission cross-sections. On the negative side, they offer only modest thermal conductivity, $\sim 3 \text{ W/mK}$ on the average, e.g., for $KLu(WO_4)_2$ (KLuW) [1], which makes them more suitable for low to medium laser power levels. The above advantages have been widely utilized in Nd, Yb, and Tm lasers but not fully exploited in Ho lasers operating on their main $^5I_7 \rightarrow ^5I_8$ transition slightly above $2 \mu\text{m}$. This can be attributed to the poor availability of suitable pump sources (laser diodes or Tm-fiber lasers) at the corresponding absorption maximum ($\sim 1961 \text{ nm}$) for in-band excitation to the 5I_7 Ho³⁺ electronic state, the only way of resonant pumping the Ho³⁺ active ion, leading to minimum thermal load due to non-radiative relaxation processes.

In particular, for passively mode-locked (ML) lasers, Nd-doped and Yb-doped $KM(WO_4)_2$ crystals performed very well due to their relatively broad gain bandwidths. In the $2 \mu\text{m}$ range, however, due to the relatively weak ligand fields, Tm-doped $KM(WO_4)_2$ crystals emit below $2 \mu\text{m}$, and the structured water vapor air absorption prevents operation in the sub-100 fs regime. The shortest pulses of 141 fs were obtained from a Tm:KLuW laser ML by single-walled carbon nanotubes (SWCNTs), by shifting the central wavelength to 2037 nm using a selective output coupler (OC), which inevitably restricts the actual gain bandwidth [2]. Attempts to mode-lock the codoped Tm,Ho:KLuW laser emitting above $2 \mu\text{m}$ using SWCNTs [3] or semiconductor saturable absorber mirrors (SESAMs) [4] produced only picosecond pulses. Therefore, the study of singly Ho-doped $KM(WO_4)_2$ crystals for ML lasers is justified by the expected higher intracavity intensities at reduced thermal load under in-band excitation into the upper laser level, which will favor the realization of soliton-like regimes.

In the case of the Ho³⁺ ion, matching of the ionic radii with the passive rare-earth host component, necessary for effective active ion doping and high optical quality of the grown crystals, is best for $M = Y$ and equally good for $M = Gd$ and Lu . A direct comparison employing the same pump sources (fiber-coupled GaSb-based laser diodes at 1941 nm and a diode-pumped Tm:KLuW laser emitting at 1946 nm) showed similar performance of 3 at. % doped crystals [5]. The maximum output

power achieved from a continuous-wave (CW) Ho:KLuW laser reached 648 mW at 2078 nm under 1946 nm pumping [6]. With a quantum defect of only 6%, the efficiency in this short near-hemispherical cavity laser reached 31.6% with respect to the absorbed pump power. Slope efficiency as high as 84% was achieved with Ho:KLuW in a microchip configuration, the highest for an in-band-pumped Ho laser [7]. However, CW output powers exceeding 1 W have been demonstrated only with a special design, a thin-disk 3 at. % Ho : KY(WO₄)₂/KY(WO₄)₂ epitaxial laser: in this case, the 250 μm thick active layer was pumped in four passes (simple retroreflection) by a Tm-fiber laser near 1960 nm, emitting 1.57 W at 2057 nm [8].

In the present work, we studied 3.9 at. % Ho:KLuW in a standard, long and folded cavity with tight focusing suitable for the integration of mode-locking elements under in-band pumping by an unpolarized Tm-fiber laser. By employing double-pass pumping, we demonstrate, for the first time, a multi-watt output power level in the true CW regime.

2. EXPERIMENTAL SETUP

The absorption and emission cross-sections for the main Ho³⁺ transition to the ground level in KLuW are shown in Fig. 1(a) for the strongest $E//N_m$ polarization [9]. Here, N_m denotes the principal optical axis corresponding to the medium refractive index. This transition corresponds to a quasi-three-level laser scheme with reabsorption. The maximum absorption cross-section amounts to $\sigma_a = 1.44 \times 10^{-20} \text{ cm}^2$ near 1961 nm, with a bandwidth (FWHM) of $\sim 10 \text{ nm}$ [5]. The maximum emission cross-section amounts to $\sigma_e = 2.45 \times 10^{-20} \text{ cm}^2$ near 2059 nm [5].

Due to the high cross-sections, the Ho³⁺ lifetime in KLuW is relatively short. At a doping level of 3% in the growth charge (corresponding to an actual concentration of 3.9% or an ion density of $N = 2.54 \times 10^{20} \text{ cm}^{-3}$ in the grown crystal), the measured fluorescence lifetime of 8.4 ms was obviously affected by reabsorption, while the radiative lifetime calculated by averaging the emission cross-sections for the three polarizations, 5.38 ms, was rather close to the 5.8 ms measured for 1% Ho-doping in the charge (1.4% actual doping or $N = 9.31 \times 10^{19} \text{ cm}^{-3}$) [9].

The product of the maximum emission cross-section near 2059 nm and the radiative lifetime, often used as a figure of merit when comparing different materials, amounts to $\sim 1.32 \times 10^{-19} \text{ cm}^2 \cdot \text{ms}$ for $E//N_m$, and is exceptionally high, partly due to the strong anisotropy of this monoclinic crystal. The high cross-sections normally result in bleaching of the absorption in cavities with tight focusing, as those used for ML lasers. Relatively short lifetimes are, on the other hand, advantageous in mode-locked lasers since this increases the stability against parasitic Q-switching.

In quasi-three-level laser systems, the oscillation wavelength is predicted by the gain cross-section $\sigma_g = \beta\sigma_e - (1 - \beta)\sigma_a$, where β is the population inversion rate. We have calculated this cross-section for $E//N_m$ in Fig. 1(b) for realistic values of the inversion rate. As can be seen, oscillation wavelengths near 2078 nm are expected at low inversion rates, experiencing some blue shift at higher output coupling, which will correspond to a higher inversion rate in the steady-state CW regime.

For $\beta > 0.22$, the main maximum near 2059 nm becomes dominant.

The cuboid sample of Ho:KLuW used in the present experiment had dimensions of 2.97 mm (N_g) \times 2.86 mm (N_m) \times 3.01 mm (N_p) along the orthogonal axes of the optical ellipsoid, with all six faces polished to laser quality. Light polarization parallel to N_g and N_p corresponds to the maximum and minimum refractive indices, respectively. The actual doping level in the crystal was 3.9%. The sample was inclined at Brewster's angle for N_m polarization, which exhibits the highest absorption and emission cross-sections (see Fig. 2). The beam propagation was close to the N_p direction, which coincides with the

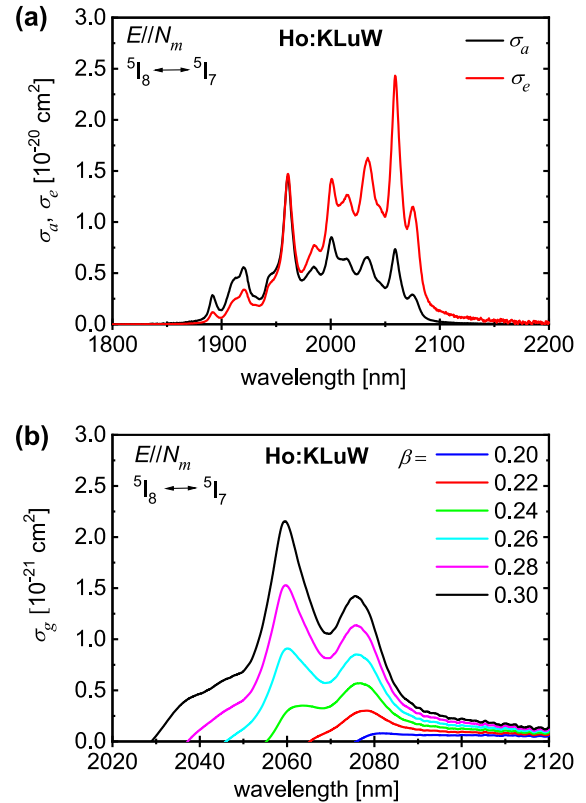


Fig. 1. (a) Absorption (σ_a) and emission (σ_e) cross-sections for Ho:KLuW in the strongest N_m -polarization, and (b) calculated gain cross-sections for the same polarization at different inversion rates β .

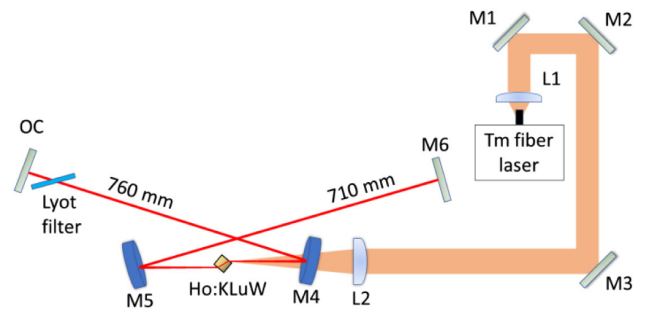


Fig. 2. Experimental setup of the in-band-pumped Ho:KLuW laser. L1, aspherical anti-reflection (AR)-coated collimating lens (focal length: $f = 11 \text{ mm}$); L2, best form AR-coated focusing lens ($f = 75 \text{ mm}$); M1, M2, and M3, pump bending mirrors; M4 [high reflection (HR) laser, high transmission (HT) pump] and M5 (HR laser and pump), folding focusing mirrors; M6 (HR laser, HT or HR pump), plane mirror; and OC, plane output coupler.

monoclinic b axis of KLuW, being normal to one of the natural crystal faces. Thus, although the ~ 1959 nm pump beam was unpolarized, the horizontal component parallel to N_m was predominantly absorbed due to the strong reflection of s -polarized light and the lower absorption cross-section for N_g polarization [9].

The Ho:KLuW sample was mounted using indium foil for better thermal contact on all four lateral surfaces in a standard copper holder with water cooling at 12°C . The latter was placed between two concave folding mirrors, M4 and M5, with a radius of curvature, $\text{RoC} = -100$ mm, as shown in Fig. 2. The pump beam in the laser crystal had a waist (radius) of $\sim 15 \mu\text{m} \times 30 \mu\text{m}$ in the sagittal and tangential planes, respectively, smaller than the corresponding calculated values for the laser waist (radius) of $\sim 28 \mu\text{m} \times 48 \mu\text{m}$.

Different OCs with a transmission at the laser wavelength T_{OC} in the range of 0.2%–5% were available. A Lyot filter (2 mm thick quartz plate) could optionally be inserted at Brewster's angle close to the OC for wavelength tuning. A spatially single-mode, narrowband (<1 nm), Tm-fiber laser (Model IFL15, LISA Laser Products, OHG), delivering a maximum power of 11.5 W, was used as a pump source. Its emission wavelength varied between 1958 and 1959 nm with increasing power. In view of the close pump and laser wavelengths, we opted for an M5 mirror reflecting both of them for easier cavity alignment. Using plane rear mirrors M6 reflecting only the laser or both the laser and pump beams, it was possible to compare single- and double-pass pumping while maintaining operation in the fundamental transversal mode. Double-pass pumping helps increase the absorption in the presence of bleaching and ensures a more homogeneous distribution of the thermal load to avoid crystal fracture.

We measured the low-signal transmission of the Ho:KLuW sample with an unfocused pump beam at normal incidence and obtained 23.7% for $E//N_m$ and 38.9% for $E//N_g$. This is in very good agreement with the $\sim 25\%$ calculated from the spectroscopic data for $E//N_m$, taking into account the Fresnel reflections of the uncoated sample.

3. EXPERIMENTAL RESULTS

It is well known that the Ho-doping level in crystals or ceramics is limited for laser applications due to a few factors. In-band pumping, in the absence of Tm-codoping, alleviates some of the resonant interactions in the excited states; however, energy transfer upconversion remains as a detrimental limiting factor, further increasing the heat load at higher doping levels, in addition to the expected concentration quenching, which has not been quantified for KLuW [9]. Both effects are expected to be somewhat suppressed in KLuW due to the relatively large ion–ion separations, and the optimum doping levels are expected to be higher compared to other host crystals. Thus, the conclusion in Ref. [10] was that actual doping levels of 4%–6%, depending on the thickness, are optimum for KLuW under in-band pumping. The limited doping level and the non-optimum pump wavelength (commercial Tm-fiber lasers are mostly adapted for pumping Ho:YAG or Ho:YLF lasers) may lead to low absorption efficiency, even for the $\text{KM}(\text{WO}_4)_2$ hosts. Thus, double-pass pumping by retroreflecting the pump

beam has been widely used in such lasers, not only in the thin-disk design [8] but also in most of the short-cavity mini or microchip lasers employing bulk crystals at normal incidence [5–7,9–11]. In contrast to 800 nm pumping of codoped crystals [3,4], this could be realized without additional mirrors, using the same cavity mirrors, basically the OC. Since feedback to the Tm:KLuW pump laser was observed in some cases, also intracavity pumping of Ho:KLuW has been suggested as a viable alternative for microchip lasers [12].

We established that using an optimized pump wavelength, close enough to the oscillation wavelength, double-pass pumping without an additional retroreflecting pump mirror is also possible in long cavities with Brewster angle geometry for the laser crystal, which are suitable for mode-locking. In the present setup, we did not observe any feedback to the Tm-fiber pump laser as a result of such a retroreflection (easily detectable by the weak feedback from L2 or M4 in Fig. 2).

The pump power incident on the crystal could be measured in front of L2 because the transmission of this lens and the pump mirror M4 was close to 100% due to AR coatings. Reliable estimation of the absorbed pump power was, however, virtually impossible in the double pump-pass configuration due to the combined effects of bleaching, population recycling under lasing conditions, and anisotropic reflection and absorption of the unpolarized pump radiation in the Brewster-inclined Ho:KLuW sample. Thus, we present the main results below versus incident pump power instead of absorbed pump power, as in most of the previous work [5,6,9,10]. To evaluate some of these effects and to make a comparison, we first replaced the rear reflector M6 in Fig. 2 by a similar total reflector transmitting the pump radiation.

For an output coupler with $T_{\text{OC}} = 1.5\%$, the residual pump power measured behind M6 in the case of single-pass pumping increased from 1.5 W under lasing conditions to 1.95 W when lasing was interrupted near the OC, for the same incident pump level of 3.3 W. Having in mind the strong reflection of the s -polarized component of the pump light from the Brewster surfaces (roughly 40% per surface), this indicates both a strong bleaching effect under the tight focusing and a strong population recycling effect due to the intracavity laser power, which recovers the absorption toward its small-signal value.

Using the same 1.5% OC, we compared the output power at a pump level of 3.3 W for the two different M6 rear plane mirrors. While with double-pass pumping we obtained 820 mW, in the case of single-pass pumping, the output power dropped to 520 mW. Thus, all further measurements were performed under double-pass pumping, employing the M6 mirror that highly reflects both the laser and pump radiation.

The dependence of the input–output characteristics on T_{OC} with double-pass pumping is shown in Fig. 3 for incident pump powers up to 4 W. A maximum output power of 1.31 W was obtained with the 5% OC. The maximum slope efficiency with respect to the incident pump power (32.7%) was obtained for the same OC. The linear dependences in Fig. 3 indicate that effects related to the anisotropic reflection and absorption are somehow balanced under double-pass pumping. This is not unexpected since less absorption for a given polarization in the first pass will result in more absorbed power in the second one.

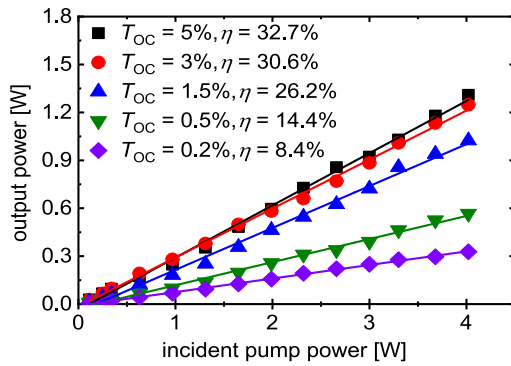


Fig. 3. Input–output characteristics of the in-band-pumped Ho:KLuW laser for $E//N_m$ and different output couplers. η is the slope efficiency with respect to the incident pump power at ~ 1959 nm.

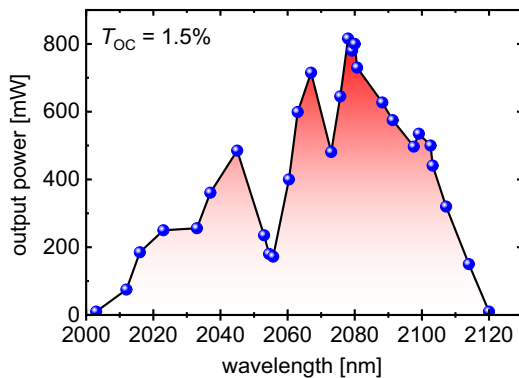


Fig. 4. Tuning performance of the in-band-pumped Ho:KLuW laser with double-pass pumping at an incident pump power of 3.3 W.

The emission wavelength was almost constant for all OCs, decreasing only from about 2080 to 2078 nm when increasing the output coupling, which increases the inversion level under CW operation.

Figure 4 shows the tuning performance obtained at a pump power of 3.3 W with the Lyot filter for the 1.5% OC. After careful alignment of the birefringent filter, the maximum output power was almost the same as without it (cf. Fig. 3). The tuning range extended from 2003 to 2120 nm, i.e., roughly 117 nm at the zero output level. The tuning curve behavior correlates with the emission and gain cross-sections. This can be clearly seen from the maximum in Fig. 4, which is at the same position as the free oscillation wavelength without the Lyot filter in the cavity. The power drop near 2050 nm corresponds to a local minimum in the emission cross-section in Fig. 1(a), but there is no such minimum in the gain cross-section in Fig. 1(b).

The power scaling performance of the crystal was studied using a chopper for the pump beam with a rotation frequency of 50 Hz and an aspect ratio of 1:1. This ensures that the pump period is longer than the fluorescence lifetime. We used the optimum output coupler of 5%. The maximum output power in quasi-CW operation reached 2.82 W. Without using the chopper, it dropped only slightly to 2.7 W at 2078 nm for the same maximum level of 8 W for the incident pump power. The slope efficiencies were also very close, reaching 33.5% with respect to

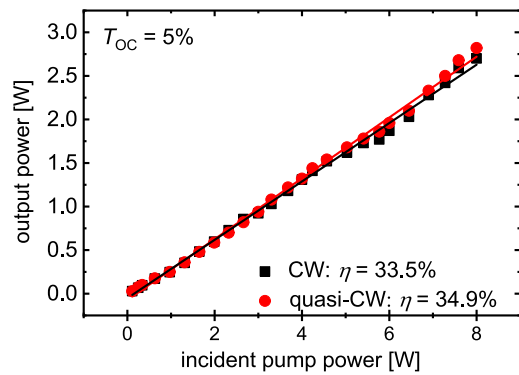


Fig. 5. Power scaling using double-pass pumping with $T_{OC} = 5\%$ in the quasi-CW (circles and line) and true CW (squares and line) regimes. η is the slope efficiency relative to the incident pump power.

the incident pump power in true CW operation. Once thermal equilibrium was established, the long-term stability in the true CW regime at maximum power was better than $\pm 1\%$.

Even at such pump levels, no damage was observed in the laser crystal after long-term operation. Also, almost no roll-off is seen in Fig. 5. The marginal difference between quasi-CW and true CW performance indicates negligible thermal effects. From the residual pump power measured without double-pass pumping, we can estimate that the slope efficiency calculated versus absorbed pump power in the case of double-pass pumping will be at least 2 times higher compared to the values presented versus incident power.

4. CONCLUSION

To conclude, we demonstrated a true CW output of 2.7 W from an in-band-pumped 3.9 at. % Ho:KLu(WO₄)₂ laser. This doping level seems optimum to suppress unwanted processes in the Ho³⁺-ion energy level scheme and simultaneously ensures sufficient absorption and reduced risk of fracture. Double-pass pumping has the potential to increase the absorption and the laser efficiency, and simultaneously homogenize the thermal load, possibly helping to suppress optical damage effects. Further improvement of the present results is expected using polarized pump sources near 1960 nm. The high intracavity powers achieved are promising for the realization of Kerr-lens soliton-type mode-locking by adding cavity elements with negative group-velocity dispersion. Mode-locking using saturable absorbers, such as SESAM for self-starting, is also feasible in the present setup since double-pass pumping can be realized also by the OC due to the close pump and laser wavelengths. We also tested that the incorporation of dispersive mirrors for negative group-velocity dispersion is compatible with double-pass pumping since they also reflected the pump light.

Funding. Deutsche Forschungsgemeinschaft (M-0040); European Social Fund Plus (2022FI_B200021, 2021FI_B100170, 2020FI_B00522); Ministerio de Ciencia, Innovación y Universidades (MICIU/AEI/10.13039/501100011033/FEDER/UE).

Acknowledgment. Xavier Mateos is a Serra Hünter Fellow, Spain.

Disclosures. The authors declare no conflicts of interest.

Data availability. Data underlying the results presented in this paper are not publicly available at this time but may be obtained from the authors upon reasonable request.

REFERENCES

1. O. Silvestre, J. Grau, M. C. Pujol, *et al.*, "Thermal properties of monoclinic $\text{KLu}(\text{WO}_4)_2$ as a promising solid state laser host," *Opt. Express* **16**, 5022–5034 (2008).
2. A. Schmidt, S. Y. Choi, D.-I. Yeom, *et al.*, "Femtosecond pulses near 2 μm from a Tm:KLuW laser mode-locked by a single-walled carbon nanotube saturable absorber," *Appl. Phys. Express* **5**, 092704 (2012).
3. V. Aleksandrov, A. Gluth, V. Petrov, *et al.*, "Tm,Ho:KLu(WO₄)₂ laser mode-locked near 2 μm by single-walled carbon nanotubes," *Opt. Express* **22**, 26872–26877 (2014).
4. V. Aleksandrov, A. Gluth, V. Petrov, *et al.*, "Mode-locked Tm,Ho:KLu(WO₄)₂ laser at 2060 nm using InGaSb-based SESAMs," *Opt. Express* **23**, 4614–4619 (2015).
5. V. Jambunathan, X. Mateos, M. C. Pujol, *et al.*, "Continuous-wave laser generation at $\sim 2.1 \mu\text{m}$ in Ho:KRE(WO₄)₂ (RE= Y, Gd, Lu) crystals: a comparative study," *Opt. Express* **19**, 25279–25289 (2011).
6. X. Mateos, V. Jambunathan, M. C. Pujol, *et al.*, "CW lasing of Ho in $\text{KLu}(\text{WO}_4)_2$ in-band pumped by a diode-pumped Tm:KLu(WO₄)₂ laser," *Opt. Express* **18**, 20793–20798 (2010).
7. P. Loiko, J. M. Serres, X. Mateos, *et al.*, "In-band-pumped Ho:KLu(WO₄)₂ microchip laser with 84% slope efficiency," *Opt. Lett.* **40**, 344–347 (2015).
8. X. Mateos, S. Lamrini, K. Scholle, *et al.*, "Holmium thin-disk laser based on Ho:KY(WO₄)₂/KY(WO₄)₂ epitaxy with 60% slope efficiency and simplified pump geometry," *Opt. Lett.* **42**, 3490–3493 (2017).
9. V. Jambunathan, X. Mateos, M. C. Pujol, *et al.*, "Crystal growth, optical spectroscopy, and continuous-wave laser operation of Ho:KLu(WO₄)₂ crystals," *Appl. Phys. B* **116**, 455–466 (2014).
10. V. Jambunathan, X. Mateos, M. C. Pujol, *et al.*, "Optimization of dopant concentration in Ho:KLu(WO₄)₂ laser achieving $\sim 70\%$ slope efficiency," *Laser Phys.* **23**, 125801 (2013).
11. P. Loiko, J. M. Serres, X. Mateos, *et al.*, "Ho:KLu(WO₄)₂ microchip laser Q-switched by a PbS quantum-dot-doped glass," *IEEE Photonics Technol. Lett.* **27**, 1795–1798 (2015).
12. J. M. Serres, P. A. Loiko, X. Mateos, *et al.*, "Ho:KLuW microchip laser intracavity pumped by a diode-pumped Tm:KLuW laser," *Appl. Phys. B* **120**, 123–128 (2015).